

# HIGH PRESSURE VAPOR + LIQUID + LIQUID EQUILBRIA OF SOME CARBON DIOXIDE + ORGANIC + WATER TERNARY SYSTEMS

**Michael J. Lazzaroni, David Bush, Jason P. Hallett, James S. Brown,  
Charles L. Liotta, and Charles A. Eckert**

School of Chemical Engineering and Specialty Separations Center  
Georgia Institute of Technology, *Atlanta, GA, USA*

**Roger Gläser**

Institute of Chemical Technology, University of Stuttgart, *Germany*

## Abstract

Supercritical carbon dioxide, although an inert diluent, can increase rates and/or selectivity for both homogeneous and heterogeneous catalyzed reactions and improve recovery of homogenous catalysts. For reactions that involve permanent gases (e.g. O<sub>2</sub>, CO, and H<sub>2</sub>) and liquids, addition of carbon dioxide can improve the mutual solubility and lower resistance to mass transfer. In homogeneous catalyzed reactions, the catalyst can be tuned to be soluble or insoluble with carbon dioxide present, thus allowing for high catalyst recovery.

High pressure phase equilibria for the systems containing carbon dioxide, an organic (tetrahydrofuran, acetonitrile, or 1,4-dioxane), water, were measured using a variable-volume sapphire tube. Using total volumes measurements and known added mass, we can calculate compositions and density in both phases. This provides for rapid and facile measurement with no sampling or calibration. We have found that these systems are predicted well with the Peng-Robinson Equation of State with Wong-Sandler mixing rules from correlations of the binary systems. Applications of the phase behavior on reaction conditions and separations are addressed.

## Introduction

Supercritical carbon dioxide, although an inert diluent, can increase rates and/or selectivity for both homogeneous and heterogeneous catalyzed reactions and improve recovery of homogenous catalysts. For reactions that involve permanent gases (e.g. O<sub>2</sub>, CO, and H<sub>2</sub>) and liquids, addition of carbon dioxide can improve the mutual solubility and lower resistance to mass transfer.

In homogeneous catalysis, we take advantage of the unique phase behavior of CO<sub>2</sub>. CO<sub>2</sub> is the only nontoxic, nonflammable solvent that is miscible with fluorocarbons, hydrocarbons, and most polar organics like alcohols, ethers, ketones, and nitriles, but is immiscible with water. For fluorine-organic biphasic chemistry [1], CO<sub>2</sub> can be added to run these reactions homogeneously with improved reaction rates [2]. CO<sub>2</sub> can also be used to improve water-organic biphasic chemistry. The traditional water/organic biphasic technique, popularized by the Ruhrchemie/Rhône-Poulenc process [3] requires a water-insoluble solvent, which is required to recycle the catalyst, but hinders mass transfer. Here the addition of a polar organic co-solvent coupled with subsequent phase splitting induced by the dissolution of gaseous carbon dioxide creates the opportunity to run homogeneous reactions in an organic/aqueous mixture with a

water-soluble catalyst. After CO<sub>2</sub>-induced phase separation, the catalyst-rich aqueous phase and the product-rich organic phase can be easily decanted and the aqueous catalyst recycled.

To investigate the feasibility of these processes, vapor-liquid-liquid phase equilibria in mixtures of water + CO<sub>2</sub> + tetrahydrofuran, 1,4-dioxane, or acetonitrile were studied at 25°, 40°, and 60° C and pressures ranging from 10 to 57 bar.

## Experimental Methods

**Materials.** HPLC grade tetrahydrofuran (99%), 1,4 dioxane (99%), acetonitrile (99%), and water (99%) were obtained from Aldrich Chemical Co. and were used as received. SFC Grade carbon dioxide (99.99%) was obtained from Matheson Gas Products. The CO<sub>2</sub> was further purified to remove trace water using a Matheson (Model 450B) gas purifier and filter cartridge (Type 451).

**Apparatus.** Figure 1 shows a schematic of the equilibrium cell apparatus. The equilibrium cell consists of a hollow sapphire cylinder (50.8 mm O.D. × 25.4±0.0001 mm I.D. × 203.2 mm L) with a movable stainless steel piston inside and stainless steel end caps. The cell is divided into two chambers separated by an o-ring seal on the piston with one side containing the equilibrium components and the other side containing the pressuring fluid, in this case water. An air bath maintains constant temperature in the cell to within ±0.2 K.

The liquid phase compounds are added to the cell using a gas-tight syringe. The syringe was weighed before and after liquid addition to find mass added. CO<sub>2</sub> was added to the cell from a syringe pump running at constant pressure and temperature. Using the volume displacement of the syringe and the Span-Wagner EoS, the moles of CO<sub>2</sub> added to the cell is calculated.

Liquid and vapor volumes are calculated by measuring the height of the meniscus with a micrometer cathetometer. For displacements less than 50 mm, the accuracy is 0.01 mm; for larger displacements, the accuracy is 0.1 mm.

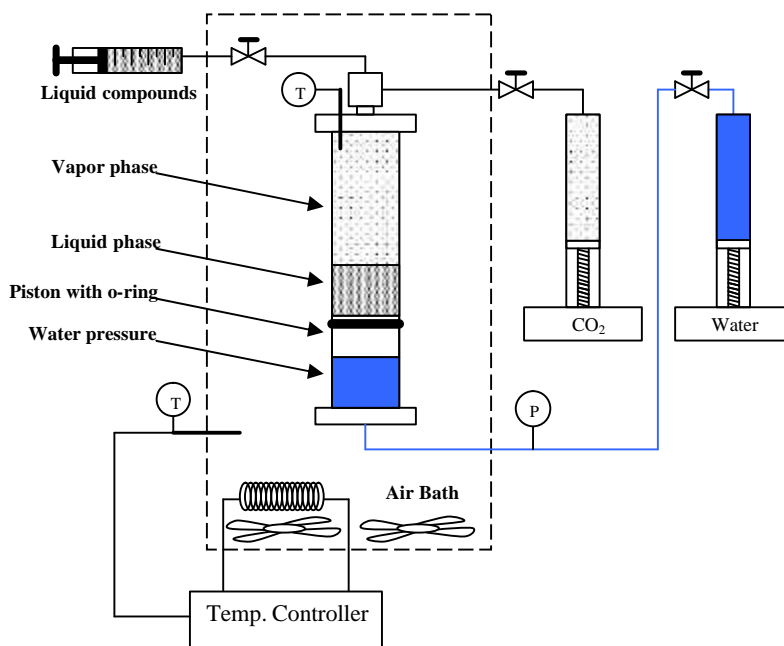


**Figure 1.** Schematic of equilibrium cell apparatus.

**Experimental procedure.** The procedure followed for measuring the phase equilibria of the ternary system is similar to that of Renon et al. [4] In short, with 3 components, 3 phases, and a fixed temperature and pressure, there are 0 degrees of freedom; thus, the concentration of each phase will be independent of the overall concentration. A minimum of three loadings of different compositions is necessary to calculate the composition and molar volumes of the three phases from the measured volumes of each phase and the overall composition. In this experiment, five loadings were performed for greater precision.

Additionally, the composition and molar volume of the vapor phase were assumed from known data. Since one of the liquid phases is mostly water, the partial pressure of water in the vapor phase was assumed to be the vapor pressure, and the composition of the other two components was predicted from correlated binary data. The molar volume of the vapor phase was assumed to be that of pure CO<sub>2</sub>, since the composition is never less than 98% CO<sub>2</sub>.

## Experimental Results

The high pressure phase vapor–liquid–liquid equilibria of carbon dioxide + tetrahydrofuran (THF) + water were measured at 298.15 K, 313.15 K, 333.15 K and at pressures from 10 to 52 bar. Composition and molar volume results are shown in Table 1. The composition of the vapor phase is not shown in the tables.

The high pressure phase vapor–liquid–liquid equilibria of carbon dioxide + acetonitrile (ACN) + water were measured at 313.15 K and at pressures from 18.6 to 52 bar. Composition and molar volume are shown Table 2.

The high pressure phase vapor–liquid–liquid equilibria of carbon dioxide + 1,4-dioxane (DIOX) + water were measured at 313.15 K and at pressures from 27.7 to 57 bar. Composition and molar volume are shown Table 3.

**Table 1.** Carbon Dioxide + Tetrahydrofuran + Water System at 298, 313, and 333 K.

$T$ (K)	$P$ (bar)	Liquid phase 1 (L <sub>1</sub> )				Liquid phase 2 (L <sub>2</sub> )				Vapor
		$x_{\text{CO}_2}$	$x_{\text{THF}}$	$x_{\text{H}_2\text{O}}$	$v_L$ (cm <sup>3</sup> /mol)	$x_{\text{CO}_2}$	$x_{\text{THF}}$	$x_{\text{H}_2\text{O}}$	$v_L$ (cm <sup>3</sup> /mol)	$v_V$ (cm <sup>3</sup> /mol)
298	10.3	0.005	0.136	0.859	23.6	0.085	0.492	0.423	58.2	2267.6
298	20.7	0.014	0.076	0.910	20.9	0.300	0.542	0.158	61.8	1065.0
298	31.0	0.049	0.049	0.902	19.4	0.436	0.461	0.103	62.1	658.8
298	41.4	0.057	0.039	0.904	19.4	0.657	0.295	0.048	54.1	449.4
298	51.7	0.054	0.020	0.926	17.1	0.847	0.142	0.011	54.0	316.0
313	9.9	0.012	0.118	0.870	25.1	0.045	0.511	0.445	53.4	2512.6
313	24.2	0.028	0.072	0.901	22.1	0.216	0.520	0.264	58.3	957.9
313	38.6	0.016	0.045	0.939	20.2	0.437	0.445	0.119	60.3	549.5
313	44.9	0.011	0.044	0.945	20.3	0.568	0.384	0.049	60.8	451.9
313	52.1	0.030	0.033	0.937	19.9	0.625	0.324	0.051	59.1	367.4
333	10.3	0.000	0.095	0.905	23.9	0.037	0.600	0.364	58.2	2584.0
333	20.7	0.003	0.058	0.939	22.3	0.131	0.597	0.272	55.5	1240.7
333	31.0	0.001	0.043	0.955	21.0	0.224	0.573	0.202	59.2	791.1
333	41.4	0.021	0.040	0.939	20.5	0.306	0.548	0.146	64.6	565.3
333	51.7	0.004	0.006	0.990	20.4	0.424	0.482	0.094	58.0	428.6

**Table 2.** Carbon Dioxide + Acetonitrile + Water System at 313 K

$T$ (K)	$P$ (bar)	Liquid phase 1 ( $L_1$ )				Liquid phase 2 ( $L_2$ )				Vapor
		$x_{CO_2}$	$x_{ACN}$	$x_{H_2O}$	$v_L$ ( $cm^3/mol$ )	$x_{CO_2}$	$x_{ACN}$	$x_{H_2O}$	$v_L$ ( $cm^3/mol$ )	$v_V$ ( $cm^3/mol$ )
313	18.6	0.038	0.229	0.733	25.7	0.076	0.435	0.489	33.6	1283.7
313	24.1	0.019	0.136	0.845	21.0	0.170	0.594	0.237	42.7	960.6
313	31.0	0.010	0.067	0.924	20.1	0.258	0.624	0.119	44.1	717.9
313	41.4	0.011	0.082	0.907	18.0	0.407	0.527	0.066	49.7	503.0
313	51.7	0.025	0.056	0.918	18.7	0.495	0.434	0.071	46.6	370.9

**Table 3.** Carbon Dioxide + 1,4-Dioxane + Water System at 313 K

$T$ (K)	$P$ (bar)	Liquid phase 1 ( $L_1$ )				Liquid phase 2 ( $L_2$ )				Vapor
		$x_{CO_2}$	$x_{DIOX}$	$x_{H_2O}$	$v_L$ ( $cm^3/mol$ )	$x_{CO_2}$	$x_{DIOX}$	$x_{H_2O}$	$v_L$ ( $cm^3/mol$ )	$v_V$ ( $cm^3/mol$ )
313	27.7	0.081	0.247	0.672	35.0	0.200	0.435	0.365	52.8	819.7
313	29.3	0.055	0.210	0.735	32.8	0.247	0.434	0.319	49.8	768.0
313	31.0	0.037	0.174	0.789	29.8	0.309	0.458	0.233	53.2	717.9
313	37.9	0.018	0.115	0.867	24.5	0.443	0.433	0.125	57.6	562.1
313	43.4	0.025	0.091	0.884	22.9	0.509	0.374	0.117	55.8	471.9
313	48.3	0.031	0.062	0.907	21.6	0.573	0.350	0.077	56.8	409.2
313	56.9	0.013	0.047	0.940	19.3	0.709	0.262	0.029	56.0	321.3

## Modeling of Experimental Results

The Peng-Robinson EoS [5] with the modification by Stryjek and Vera [6] (PRSV) was chosen to model the phase equilibrium. The pure component parameters for the PRSV are shown in Table 4. Several types of mixing rules were tried to fit the binary phase equilibria, including the two parameter van der Waals, the Mathias-Klotz-Prausnitz [7] and the Wong-Sandler [8] mixing rules. Of these mixing rules, only the Wong-Sandler (WS) rules were able to fit the water + organic phase behavior accurately. The others predicted liquid immiscibility as shown in figure 2. Both the NRTL [9] and UNIQUAC [10]  $g^E$  expressions were investigated as part of the WS mixing rules.

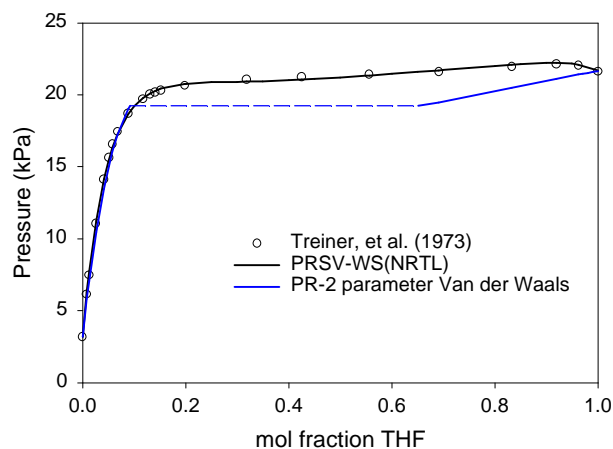


**Figure 2.** P-x diagram of the tetrahydrofuran + water binary system at 298 K with correlations of the Peng -Robinson EOS with both Wong-Sandler and a 2-parameter Van der Waals

Data for the seven constituent binary systems were collected from the literature and correlated using the PRSV-WS equation of state. Interaction parameters for the  $g^E$  model and the binary interaction parameter were fit to the data by minimizing the sum of squares error in pressure. The mixing parameters and the percent error in pressure fit are shown in table 5.

**Table 4.** Pure component parameters used in the PRSV EoS.

Compounds	$T_c$ (K)	$P_c$ (bar)	$w$	$k_1$	$r$	$q$
CO <sub>2</sub>	304.21	73.6	0.2250	0.04285	1.299	1.292
H <sub>2</sub> O	647.13	220.55	0.3438	-0.06635	0.920	1.400
tetrahydrofuran	540.15	51.9	0.2255	0.03961	2.866	2.172
acetonitrile	545.5	48.3	0.3371	-0.13991	1.870	1.724
1,4-dioxane	587	52.08	0.2793	0.02013	3.073	2.360

**Table 5.** Correlation of binary data and mixing parameters used in the PRSV-WS EoS.

System	$N_p$	T range (K)	NRTL <sup>a</sup>			UNIQUAC			Data Source
			$g_{12}/g_{21}$ <sup>b</sup>	$k_{12}$	%DP	$U_{12}/U_{21}$	$k_{12}$	%DP	
CO <sub>2</sub> + H <sub>2</sub> O	10	323	1850/2191	-0.383	3.01	1979/1308	-0.479	1.77	[11]
CO <sub>2</sub> + THF	8	313	755/-304	0.384	0.06	241/-38	0.380	0.02	[12]
THF + H <sub>2</sub> O	43	298	1649/1949	0.108	0.74	1300/-206	0.134	3.68	[13,14]
CO <sub>2</sub> + ACN	22	313	4569/-1.3	0.298	4.00	10219/-398	0.340	3.79	[15]
ACN + H <sub>2</sub> O	44	323	1106/1219	0.260	0.20	748/925	-0.104	0.26	[16,17]
CO <sub>2</sub> + DIOX	48	313	-437/984	0.338	4.84	-416/940	0.338	4.94	[15]
DIOX + H <sub>2</sub> O	113	308-323	1119/540	0.368	1.04	1032/102	-0.189	1.21	[18,19,20, 21]

<sup>a</sup>  $a = 0.36$     <sup>b</sup>  $t_{ij} = g_{ij}/RT$

## Discussion

The prediction of the type I ternary phase behavior of the CO<sub>2</sub> + THF + H<sub>2</sub>O system at temperatures of 298 K and 313 K is shown in figure 3. (Note that the compositions of only two phases are shown. The CO<sub>2</sub>-rich phase compositions were omitted because they were invariant over the temperature and pressure range studied) There is good agreement with the experimental isobaric tie-lines shown in the plot, although the predictions with the PRSV-WS using the UNIQUAC  $g^E$  model predicts a higher pressure to allow a liquid-liquid phase split than what was observed experimentally. Insufficient THF + H<sub>2</sub>O data at 313 K and the propensity for NRTL and UNIQUAC to falsely predict a phase split contributed to the poor fit at 313 K.

The prediction of the type I phase behavior of the acetonitrile and dioxane systems at 313 K are shown in figures 4 and 5 respectively. There is good agreement with experimental data in both cases, though the PRSV-WS with NRTL is able to better capture the steeper behavior in the CO<sub>2</sub>-acetonitrile system.

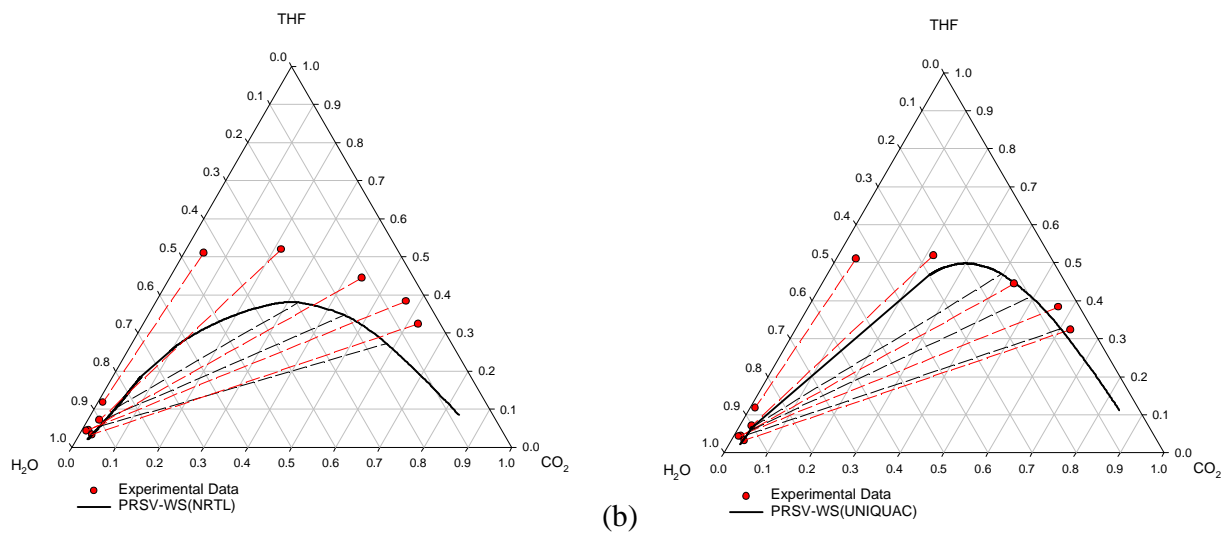
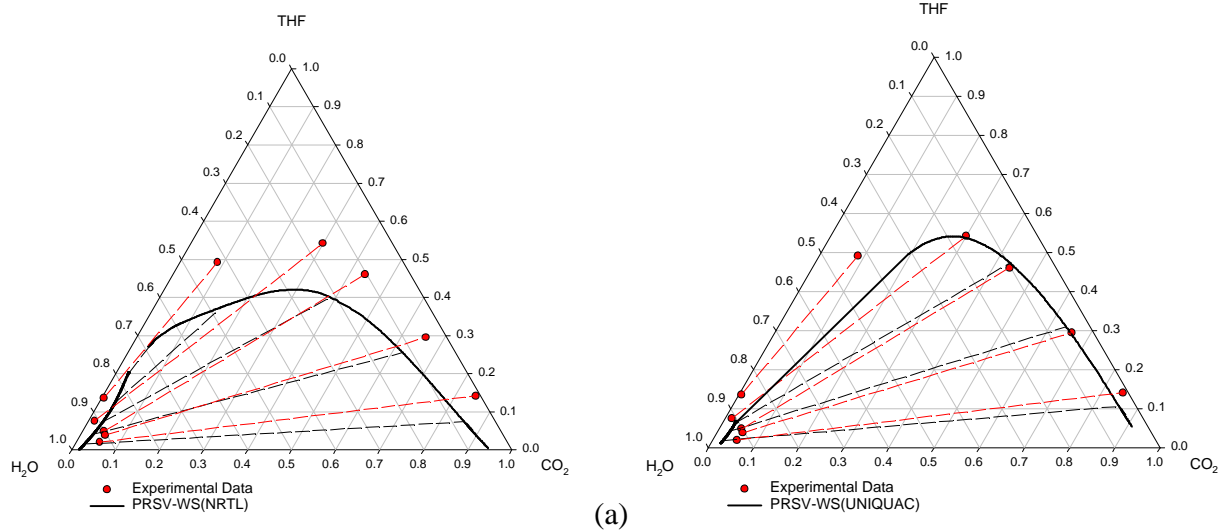


**Figure 3.** Phase behavior of CO<sub>2</sub> + tetrahydrofuran + water at (a) T=25°C. (b) T=40°C

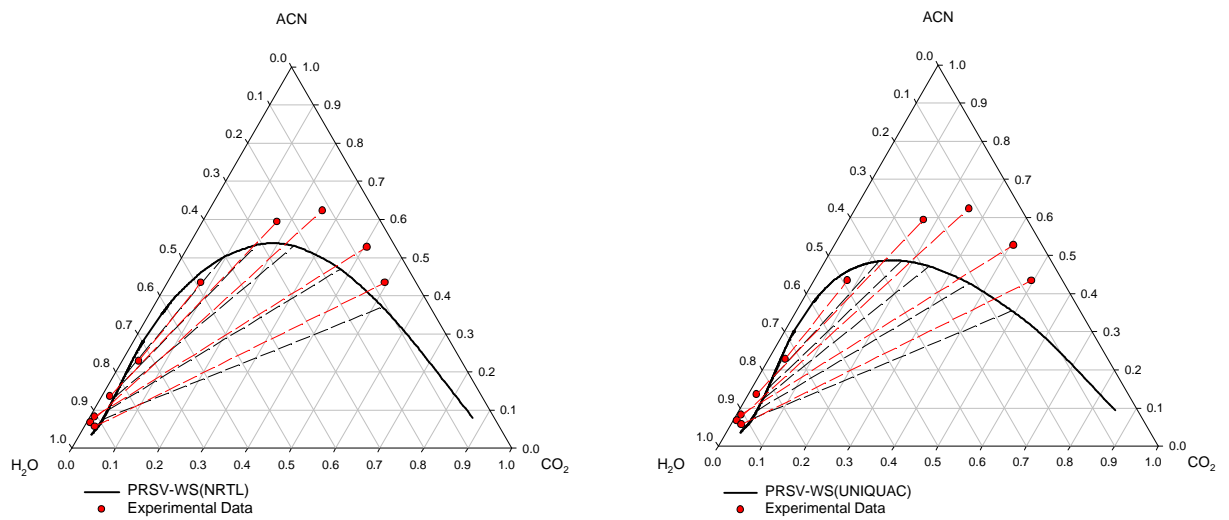


**Figure 4.** Phase behavior of CO<sub>2</sub> + acetonitrile + water at T = 40°C.

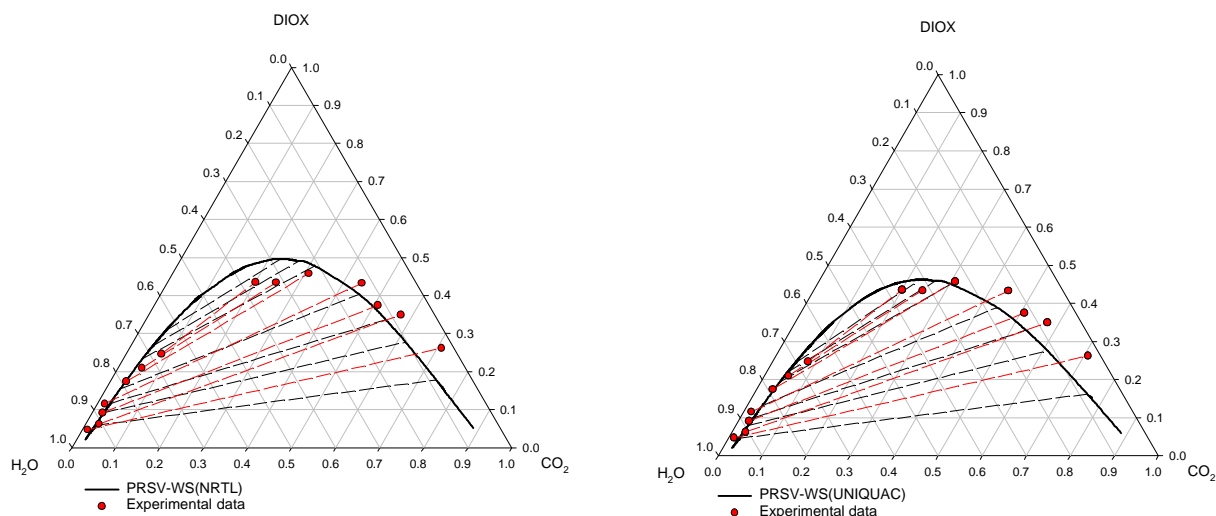


**Figure 5.** Phase behavior of CO<sub>2</sub> + dioxane + water at T = 40°C.

Figure 6 shows the measured and predicted molar volumes for the two liquid phases of the L<sub>1</sub>L<sub>2</sub>V phase equilibria at 313 K in the CO<sub>2</sub> + dioxane + water system. The prediction by the PRSV-WS(NRTL) EOS gives an error 6% from the measured molar volumes.

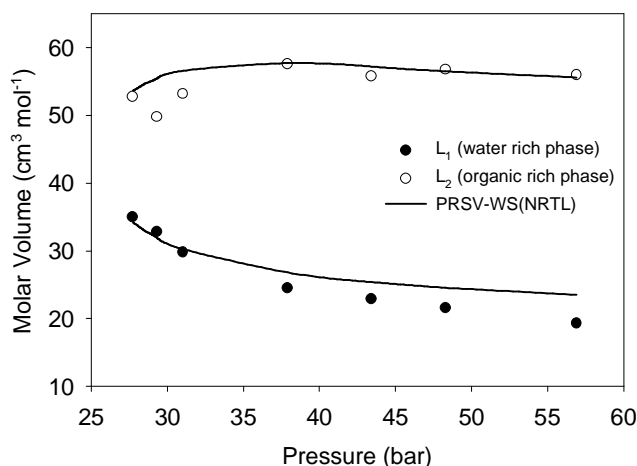


**Figure 6.** Molar volume vs. pressure for liquid phases (L<sub>1</sub>, L<sub>2</sub>) of CO<sub>2</sub> + dioxane + water system at 313 K.

## Conclusion

This experimental technique is an accurate and quick method for measuring 3 phase equilibria with no sampling or calibration. The complexity of the water+organic phase behavior requires a more complicated mixing rule. The Wong-Sandler mixing rules give reasonable predictions from binary data only.

The CO<sub>2</sub>-induced phase split of tetrahydrofuran and water appears most promising as a solvent system for the recycle of a water-soluble catalyst. Very little CO<sub>2</sub> is required to achieve a phase split, hence the separations can be run at lower pressures for lower capital and operating costs.

## References

- [1] Horváth, I. T.; Rábai, J. *Science*. 1994, 266, 72.
- [2] West, K. N.; Hallett, J. P.; Jones, R. S.; Bush, D.; Liotta, C. L.; Eckert, C.A. *J. Am. Chem. Soc.* 2003. Submitted.
- [3] Kohlpaintner, C. W.; Fischer, R. W.; Cornils, B. *Appl. Cat. A* 2001, 221, 219.
- [4] Laugier, A.; Richon, D.; Renon, H. *Fluid Phase Equilib.* 1990, 54, 19.
- [5] Peng, D. Y.; Robinson, D. B. *Ind. Eng. Chem. Fundam.* 1976, 15, 59.
- [6] Stryjek, R.; Vera, J. H. *Can. J. Chem. Eng.* 1986, 64, 323.
- [7] Mathias, P. M.; Klotz, H. C.; Prausnitz, J. M. *Fluid Phase Equilib.* 1991, 67, 31.
- [8] Wong, D. S. H.; Sandler, S. I. *Ind. Eng. Chem. Fundam.* 1992, 31, 2033.
- [9] Renon, H.; Prausnitz, J. M. *AIChE J.* 1968, 14, 135.
- [10] Abrams, D. S.; Prausnitz, J. M. *AIChE J.* 1975, 21, 116.
- [11] Bamberger, A.; Sieder, G.; Maurer, G. *J. Supercritical Fluids* 2000, 17, 97.
- [12] Lazzaroni, M. J.; Bush, D. Manuscript in preparation.
- [13] Signer, R.; Arm, H.; Daeniker, H. *Helv. Chim. Acta.* 1969, 52, 2347.
- [14] Treiner, C.; Bocquet, J. F.; Chemla, M. *J. Chim. Phys. Phys. –Chim. Biol.* 1973, 70, 72.
- [15] Kordikowski, A.; Schenk, A. P.; Van Nielen, R. M.; Peters, C. J. *J. Supercritical Fluids*. 1995, 8, 205.
- [16] Villamanan, M. A.; Allawi, A. J.; Van Ness, H. C. *J. Chem. Eng. Data.* 1984, 29, 293.
- [17] Wilson, S. R.; Patel, R. B.; Abbott, M. M.; Van Ness, H. C. *J. Chem. Eng. Data.* 1979, 24, 130.
- [18] Kortuem, G.; Valent, V. *Ber. Bunsenges. Phys. Chem.* 1977, 81, 752.
- [19] Steinbrecher, M.; Bittrich, H. J. *Z. Phys. Chem.* 1963, 224, 97.
- [20] Balcazar-Ortiz, A. M.; Patel, R. B.; Abbott, M. M.; Van Ness, H. C. *J. Chem. Eng. Data.* 1979, 24, 133.
- [21] Loehe, J. R.; Van Ness, H. C.; Abbott, M. M. *J. Chem. Eng. Data.* 1981, 26, 178.